Chronic mild hypoxia accelerates recovery from preexisting EAE by enhancing vascular integrity and apoptosis of infiltrated monocytes

Sebok K. Halder[a] and Richard Milner[a,1]

[a]Department of Molecular Medicine, The Scripps Research Institute, La Jolla, CA 92037

While several studies have shown that hypoxic preconditioning suppresses development of the experimental autoimmune encephalomyelitis (EAE) model of multiple sclerosis (MS), no one has yet examined the important clinically relevant question of whether mild hypoxia can impact the progression of preexisting disease. Using a relapsing–remitting model of EAE, here we demonstrate that when applied to preexisting disease, chronic mild hypoxia (CMH, 10% O_2) markedly accelerates clinical recovery, leading to long-term stable reductions in clinical score. At the histological level, CMH led to significant reductions in vascular disruption, leukocyte accumulation, and demyelination. Spinal cord blood vessels of CMH-treated mice showed reduced expression of the endothelial activation molecule VCAM-1 but increased expression of the endothelial tight junction proteins ZO-1 and occludin, key mechanisms underlying vascular integrity. Interestingly, while equal numbers of inflammatory leukocytes were present in the spinal cord at peak disease (day 14 postimmunization; i.e., 3 d after CMH started), apoptotic removal of infiltrated leukocytes during the remission phase was markedly accelerated in CMH-treated mice, as determined by increased numbers of monocytes positive for TUNEL and cleaved caspase-3. The enhanced monocyte apoptosis in CMH-treated mice was paralleled by increased numbers of HIF-1α+ monocytes, suggesting that CMH enhances monocyte removal by amplifying the hypoxic stress manifest within monocytes in acute inflammatory lesions. These data demonstrate that mild hypoxia promotes recovery from preexisting inflammatory demyelinating disease and suggest that this protection is primarily the result of enhanced vascular integrity and accelerated apoptosis of infiltrated monocytes.

chronic mild hypoxia | experimental autoimmune encephalomyelitis | blood–brain barrier | vascular integrity | neuroinflammation

Multiple sclerosis (MS) is the most common neurological disease affecting the young–middle age population in the United States (1, 2). MS is an inflammatory demyelinating disease in which autoreactive T lymphocytes and monocytes cross the blood–brain barrier (BBB) to invade the central nervous system (CNS; which includes the brain and spinal cord) to attack and destroy the myelin sheaths surrounding axons (demyelination). In the majority of MS patients (85%), the disease then follows a relapsing–remitting course in which the damaged myelin sheaths are repaired by endogenous remyelination that is associated with clinical remission of disease. However, with time, further demyelination occurs, resulting in clinical relapse, and eventually, many patients develop the chronic progressive form of disease, thought to be a result of myelin-deprived axons undergoing degeneration (3, 4).

Hypoxic preconditioning confers protection in several different animal models of neurological disease, including ischemic stroke and MS. In ischemic stroke, hypoxic preconditioning reduces the size of ischemic infarct and markedly reduces BBB breakdown (5–7). More recently, several studies have shown that treatment with 10% O_2 for several days (chronic mild hypoxia, CMH) suppresses the onset and progression of experimental autoimmune encephalomyelitis (EAE), an animal model of MS, both at the clinical and histopathological levels (8–10). These analyses revealed that mild hypoxic preconditioning (started before onset of EAE) reduces the extent of vascular breakdown, leukocyte infiltration, and demyelination. Our own studies revealed that CMH enhanced expression of endothelial tight junction proteins and the parenchymal vascular basement membrane protein laminin-111, but reduced levels of endothelial activation molecules such as vascular cell adhesion molecule-1 (VCAM-1), suggesting that enhancement of vascular integrity may partly explain protection afforded by CMH (10). Another study suggests that hypoxic preconditioning may suppress inflammation in EAE because CMH reduced numbers of CD4+ T lymphocytes and delayed the Th17-specific cytokine response, while increasing the numbers of regulatory T cells (Tregs) and expression of the antiinflammatory cytokine IL-10 (9). Importantly, however, no studies have yet addressed the clinically relevant question of whether mild hypoxia can improve the prognosis of preexisting EAE disease. In the current study we addressed this question in a relapsing–remitting mouse model of EAE by employing a combined clinical and histological approach.

Results

Chronic Mild Hypoxic Treatment of Preexisting EAE Accelerates Recovery at the Clinical and Histopathological Levels. EAE was induced in 10-wk-old female SJL/J mice by immunization with $PLP_{139-151}$, and once mice developed a clinical score of 2

Significance

We show that when applied to preexisting disease in the experimental autoimmune encephalomyelitis (EAE) model of multiple sclerosis, chronic mild hypoxia (CMH, 10% O_2) accelerates clinical recovery, leading to long-term stable reductions in clinical score. This was underpinned by marked reductions in histopathological markers of disease, including lower levels of vascular disruption, leukocyte accumulation, and demyelination. Mechanistically, CMH reduced vascular expression of the endothelial activation molecule vascular cell adhesion molecule (VCAM-1), but increased expression of endothelial tight junction proteins and accelerated apoptotic removal of infiltrated monocytes during the remission phase of disease. These data offer insight into the use of mild hypoxia, either as a therapeutic option for treating MS or as a tool to identify potential molecular targets.

(typically 10 to 11 d postimmunization), they were randomly assigned to normoxic (control) or chronic mild hypoxic (10% O$_2$) conditions for the duration of the experiment. As shown in Fig. 1A, in this relapsing–remitting model of EAE, normoxic mice typically reach peak clinical score after 14 d post-immunization, then several days later enter the remission phase as indicated by a declining clinical score. Interestingly, while CMH had no impact on peak clinical score, within 7 to 8 d of CMH treatment, mice showed accelerated recovery once they entered the remission phase. This resulted in marked reduction in clinical score, which first became significant around day 19 and was maintained at all timepoints thereafter (up to 35 d). Strikingly, after day 24, clinical scores of CMH-treated mice were typically 50% lower than those of normoxic controls ($P < 0.01$). Thus, CMH treatment of mice with preexisting EAE exerts a strong and sustained reduction on clinical severity.

Histological assessment of spinal cord tissue by dual-immunofluorescence (dual-IF) with the pan-leukocyte marker CD45 and the myelin stain fluoromyelin revealed that CMH-treated mice and their normoxic controls showed equivalent levels of CD45+ leukocyte infiltration in the spinal cord at peak disease (day 14) (Fig. 1B). Once mice entered the remission phase (18 to 28 d postimmunization) the extent of infiltrated CD45+ leukocytes declined considerably ($P < 0.01$ at day 21) under normoxic conditions. Importantly, however, within the spinal cords of CMH-treated mice, the number of CD45+ cells fell at a much faster rate than normoxic controls (Fig. 1 B–D). This difference first became evident after 21 d and was maintained at 28 and 35 d ($P < 0.01$ for all timepoints; Fig. 1D). Of high clinical relevance, the impact of CMH on reducing the number of CD45+ leukocytes within the spinal cord strongly correlated with preservation of myelin at all timepoints tested, including 21 ($P < 0.05$), 28 ($P < 0.01$), and 35 d ($P < 0.01$; Fig. 1 B, C, and E). Collectively, these findings demonstrate that when applied to preexisting EAE, CMH accelerates clinical recovery, leading to long-term sustained reductions in clinical score, underpinned by reduced levels of inflammatory leukocytes and long-term improvements in myelination status.

CMH Treatment of Preexisting EAE Promotes Beneficial Changes in Vascular Integrity. We recently demonstrated that hypoxic preconditioning reduces the severity of EAE, at least in part, by enhancing several different mechanisms underlying vascular integrity (10). To determine if CMH treatment of preexisting EAE induces similar effects, we first examined how CMH influences vascular integrity by performing dual-IF with the endothelial cell marker CD31 and extravascular fibrinogen leakage as a marker of vascular breakdown (Fig. 2 A and C). This revealed that at the peak phase of disease (day 14), spinal cords of normoxic and CMH mice showed equivalent levels of extensive fibrinogen leak, most notably in white matter, and this strongly colocalized with inflammatory infiltrates. However, once mice entered the remission phase, the extent of fibrinogen leak in CMH mice was far less than normoxic controls at all timepoints examined, including 21 ($P < 0.05$; Fig. 2A), 28, and 35 d (both $P < 0.01$; Fig. 2C).

CMH Suppresses Endothelial VCAM-1 Expression in EAE. During inflammation, VCAM-1 is up-regulated on activated endothelial cells and facilitates leukocyte extravasation across the BBB via interaction with the leukocyte integrin α4β1 (11). Analysis of VCAM-1 expression by CD31/VCAM-1 dual-IF revealed that while disease-free spinal cord contained only a negligible number of VCAM-1+ vessels, this number was strongly increased in mice with peak EAE (day 14) maintained under normoxic conditions (Fig. 2B). Interestingly, at this timepoint, CMH significantly reduced the number of VCAM-1+ vessels ($P < 0.05$), and this effect was maintained at the later timepoints of day 16 ($P < 0.01$), and day 21 ($P < 0.01$; Fig. 2 B and D). This suggests that

one of the earliest impacts of CMH is to reduce leukocyte infiltration into the CNS via down-regulation of endothelial–leukocyte adhesion mechanisms.

CMH Promotes Reexpression of Tight Junction Proteins. We next examined how CMH treatment of preexisting EAE influences vascular expression of ZO-1 and occludin, critical components of the BBB (12, 13). As expected, under disease-free conditions, ZO-1 and occludin tightly colocalized with CD31 on all blood vessels (Fig. 3 A and B). However, during the peak stage of EAE (day 14), the percentage of blood vessels expressing ZO-1 or occludin was dramatically reduced under both normoxic and CMH conditions ($P < 0.01$ for both proteins; Fig. 3). During clinical remission, endothelial expression of ZO-1 and occludin was largely reestablished, but interestingly, this occurred significantly faster in CMH-treated mice compared to normoxic controls (day 21: $P < 0.01$ and $P < 0.05$, day 28: $P < 0.01$ and $P < 0.01$, and day 35: $P < 0.01$ and $P < 0.05$, for ZO-1 and occludin, respectively). Thus, CMH accelerated recovery of tight junction protein expression following peak EAE, resulting in significant and sustained expression levels at all subsequent timepoints examined. In addition, because it is well established that CMH promotes a strong vascular remodeling response in the disease-free CNS (14, 15), we also quantified spinal cord vessel density and total vascular area at different timepoints to see whether this still holds true when CMH is applied on a background of full-blown inflammatory disease. As shown in Fig. 3 E and F, this revealed that compared to normoxic conditions, CMH significantly increased blood vessel density and total vascular area at all timepoints after day 21 postimmunization, including day 21 ($P < 0.01$), day 28 ($P < 0.01$), and day 35 ($P < 0.01$). Thus, even when CMH is imposed on a background of neuroinflammation, it still elicits a strong vascular remodeling response.

CMH Promotes Apoptosis of Inflammatory Leukocytes within the Inflamed Spinal Cord. Our data demonstrate that even when CMH is started after mice have developed EAE, it enhances several properties of blood vessels that contribute to vascular integrity. However, it seems unlikely that these changes in vascular properties are solely responsible for the protective effect because at peak disease (day 14 postimmunization; i.e., 3 d after CMH is started), equal numbers of infiltrated leukocytes have already entered the spinal cord of normoxic and CMH mice, but by day 21, spinal cords of CMH mice contain far fewer inflammatory leukocytes (Fig. 1 B–D). This raises two questions: what happens to leukocytes that are already in the CNS during the remission phase of disease, and why do they disappear faster in CMH-treated mice?

The currently accepted view is that following the peak phase of EAE, leukocytes within the proinflammatory CNS become exhausted and undergo apoptosis, and this decline in leukocyte numbers underlies clinical remission (16, 17). To determine whether leukocyte apoptosis is enhanced by CMH, we performed dual-IF with the pan-leukocyte marker CD45 and the apoptotic marker, cleaved caspase-3 (Fig. 4A). This revealed no cleaved caspase-3 signal under disease-free conditions, but at the peak stage of EAE (day 14) under normoxic conditions, a considerable number of CD45+ inflammatory cells within white matter lesions stained positive for cleaved caspase-3. Importantly, at this peak phase of disease, spinal cords of CMH-treated mice contained four times as many cleaved caspase-3+ leukocytes as normoxic controls ($P < 0.01$), demonstrating that CMH accelerates leukocyte apoptosis (Fig. 4B). This is well illustrated in the low-magnification images shown in Fig. 4C. We also examined leukocyte cell death at the slightly later 16-d timepoint (still in the peak phase of disease when leukocyte numbers remain high), and this confirmed that CMH increased the number of cleaved caspase-3+ leukocytes in the spinal cord at this timepoint ($P < 0.01$).
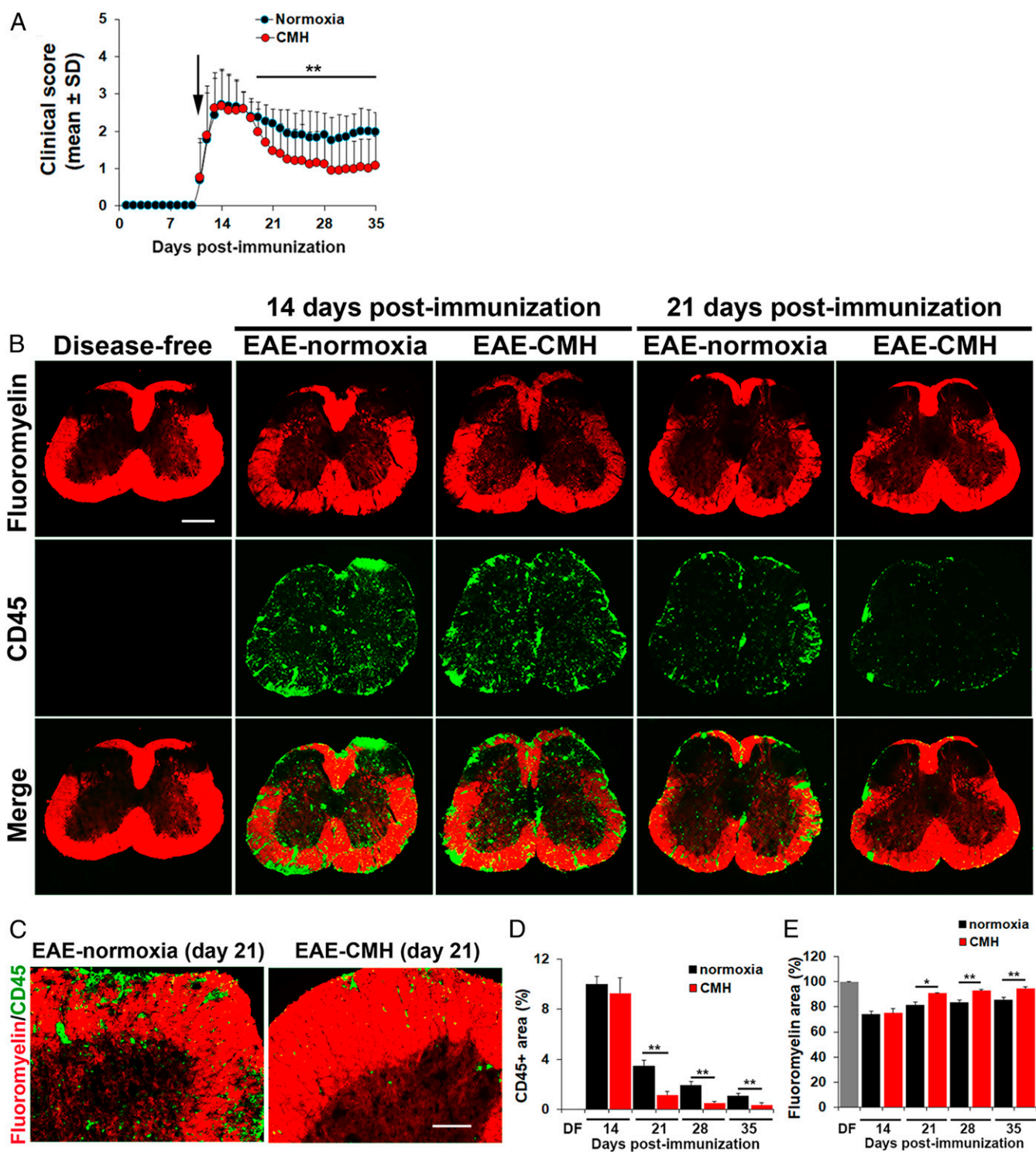
Fig. 1. Chronic mild hypoxic treatment of preexisting EAE accelerates recovery at the clinical and histopathological levels. (*A*) The impact of CMH on clinical severity of relapsing–remitting EAE. Once mice developed a clinical score of 2 (arrow), they were randomly assigned to normoxic (control) or CMH conditions, and clinical score was evaluated at daily intervals. All points represent the mean ± SD (*n* = 26–32 mice per group, cumulative of three separate experiments). Note that compared to normoxic controls, mice treated with CMH showed accelerated clinical recovery, resulting in a marked and sustained reduction in long-term clinical score. (*B* and *C*) Frozen sections of lumbar spinal cord taken from disease-free, EAE–normoxia or EAE–CMH mice at the peak and remission phases of disease (14 and 21 d postimmunization, respectively) were stained for the inflammatory leukocyte marker CD45 (AlexaFluor-488) and fluoromyelin-red. (Scale bar, 500 μm [*B*] and 100 μm [*C*].) (*D* and *E*) Quantification of CD45 (*D*) and fluoromyelin (*E*) fluorescent signal at different timepoints. Results are expressed as the mean ± SEM percent area (*n* = 6 mice per group). Note that following peak disease, CMH markedly suppressed CD45+ leukocyte load within the spinal cord and protected against demyelination. *$P < 0.05$, **$P < 0.01$.
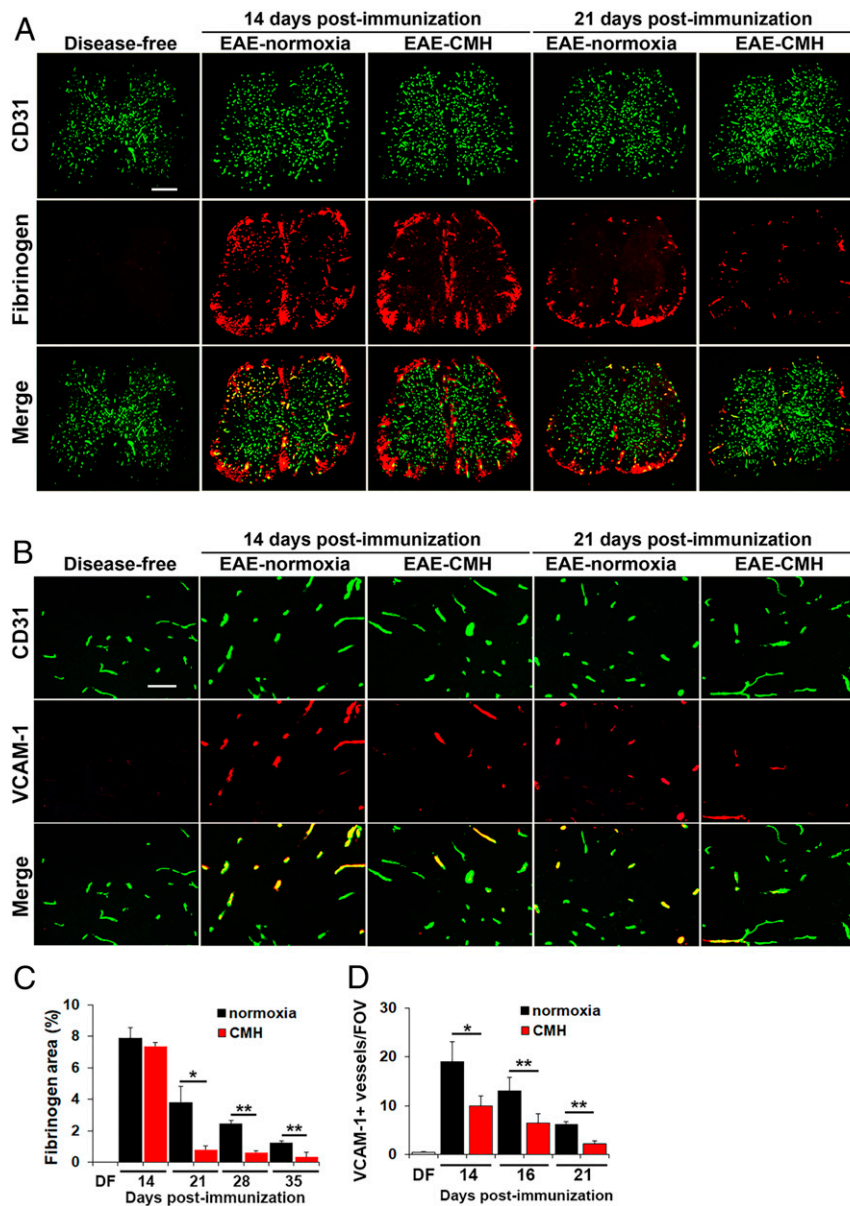
Fig. 2. CMH treatment of preexisting EAE promotes beneficial changes in vascular integrity. (*A* and *B*) Frozen sections of lumbar spinal cord taken from disease-free, EAE–normoxia or EAE–CMH mice at the peak and remission phases of disease (14 and 21 d postimmunization, respectively) were stained for CD31 (AlexaFluor-488) and fibrinogen (Cy-3) in *A* (scale bar, 500 μm) or CD31 (AlexaFluor-488) and VCAM-1 (Cy-3) in *B* (scale bar, 50 μm). (*C* and *D*) Quantification of fibrinogen leakage, expressed as the mean ± SEM percent area (*C*) and VCAM-1 expression, expressed as the mean ± SEM number of VCAM-1+ vessels/FOV (*D*). $n = 6$ mice per group. Note that following peak disease, CMH markedly suppressed fibrinogen leakage and endothelial expression of VCAM-1. *$P < 0.05$, **$P < 0.01$.

To validate these findings, we also examined leukocyte cell death using the TUNEL assay (Fig. 4*D*), and this confirmed that CMH increased the number of TUNEL+ apoptotic leukocytes within the spinal cord of mice during the peak phase of EAE, after both 14 ($P < 0.01$) and 16 d ($P < 0.05$) postimmunization (Fig. 4 *D* and *E*). Interestingly, by day 21, this pattern had reversed such that spinal cords of CMH-treated mice contained fewer TUNEL+ cells vs. normoxic mice ($P < 0.01$), consistent with our observation that at this later timepoint, CMH-treated spinal cords contain fewer leukocytes (Fig. 1*B*) because most have already undergone apoptosis.

Monocytes Are the Most Abundant Leukocyte in EAE Lesions, and CMH Preferentially Promotes Their Apoptosis. Having found that CMH accelerates leukocyte clearance from the spinal cord

during the remission phase of EAE, we next wondered if this affects all types of leukocytes or preferentially targets specific types. Leukocyte infiltrates within EAE lesions contain several different subtypes, the most well-described being CD4+ lymphocytes and Mac-1+ monocytes, with Mac-1+ monocytes the most abundant at the peak phase of disease (Fig. 5*A*), although the presence of low levels of CD8+ lymphocytes and B lymphocytes has also been implicated (18, 19). Quantification of Mac-1+ and CD4+ cell area under normoxic or CMH conditions revealed that monocytes are the most abundant type of leukocyte at all timepoints examined (days 14–28), with CD4+ cells also making a sizeable, though smaller contribution (Fig. 5 *B*–*E*). Interestingly, while CD4+ lymphocytes were fairly evenly distributed throughout white and gray matter
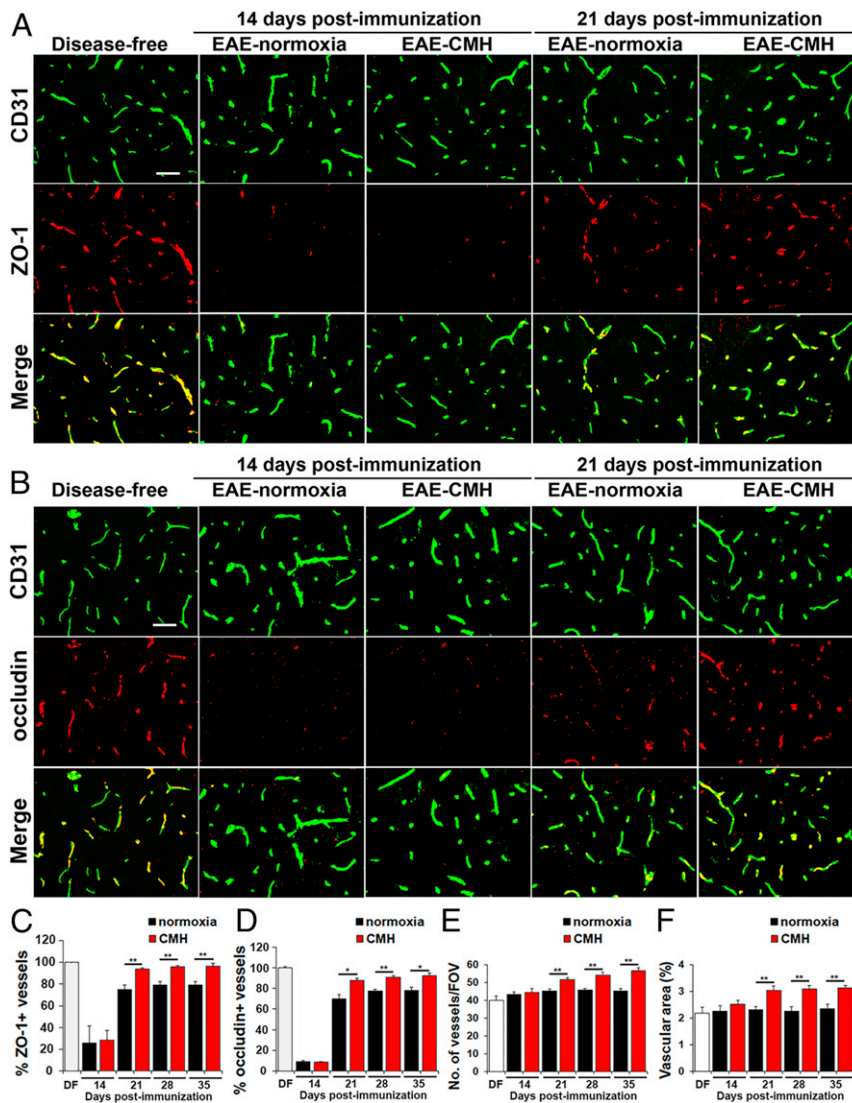
Fig. 3. CMH treatment of preexisting EAE promotes vascular remodeling and reexpression of endothelial tight junction proteins. (*A* and *B*) Frozen sections of lumbar spinal cord taken from disease-free, EAE–normoxia or EAE–CMH mice at the peak and remission phases of disease (14 and 21 d postimmunization, respectively) were stained for CD31 (AlexaFluor-488) and ZO-1 (Cy-3) in *A* or CD31 (AlexaFluor-488) and occludin (Cy-3) in *B*. (Scale bar, 50 µm.) (*C* and *D*) Quantification of ZO-1 (*C*) and occludin expression (*D*). Results are expressed as the mean ± SEM percent of vessels expressing ZO-1 or occludin. Note that during peak disease (14 d), both tight junction proteins were dramatically lost and were reexpressed during clinical remission (day 21), but at a faster rate in CMH-treated mice. (*E* and *F*) Quantification of changes in vessel density (*E*) and vascular area (*F*) during EAE progression under normoxic and CMH conditions. Results are expressed as the mean ± SEM of number of vessels/FOV or vascular area (percent of total). Note that CMH enhanced vessel density and vascular area at all timepoints from day 21 onward. $n = 6$ mice per group for all analyses. *$P < 0.05$, **$P < 0.01$.

(Fig. 5*D*), monocytes were often found in very large cellular aggregates, specifically in white matter (Fig. 5*B*). Notably, while CMH-treated mice showed a declining Mac-1+ signal as early as day 16 ($P < 0.01$; Fig. 5*C*), the CD4+ signal did not start to reduce until day 21 ($P < 0.05$; Fig. 5*E*), suggesting that CMH may have a faster and perhaps greater impact on monocyte cell death than on CD4+ lymphocytes. To determine if monocytes are specifically targeted for apoptosis by CMH, we next performed dual-IF for cleaved caspase-3 combined with either Mac-1 or CD4. This showed that the vast majority of cleaved caspase-3+ cells were Mac-1+ monocytes (Fig. 6*A*). Time-course analysis revealed that compared to normoxic conditions, CMH significantly enhanced the number of cleaved caspase-3+ monocytes at day 14 ($P < 0.01$) and day 16 ($P < 0.01$; Fig. 6*C*). In contrast, while some CD4+ lymphocytes also stained positive for cleaved caspase-3, they were

always a small minority of cleaved caspase-3+ cells, and notably, CMH had no discernible impact on the number of cleaved caspase-3/CD4 dual-positive cells (Fig. 6*D*). These data imply that CMH preferentially accelerates monocyte apoptosis during EAE remission.

CMH Enhances HIF-1α Expression Predominantly in Monocytes. Accumulating evidence shows that demyelinating lesions become acutely hypoxic during the inflammatory process (20–22), although whether hypoxia (due to vascular insufficiency) triggers inflammation or inflammation triggers hypoxia has yet to be determined. One possibility is that tissue hypoxia is the result of accumulation of large numbers of rapidly proliferating and highly metabolic inflammatory leukocytes. Based on this, we wondered if CMH treatment might be accentuating the degree of hypoxia experienced by the already hypoxic leukocytes,
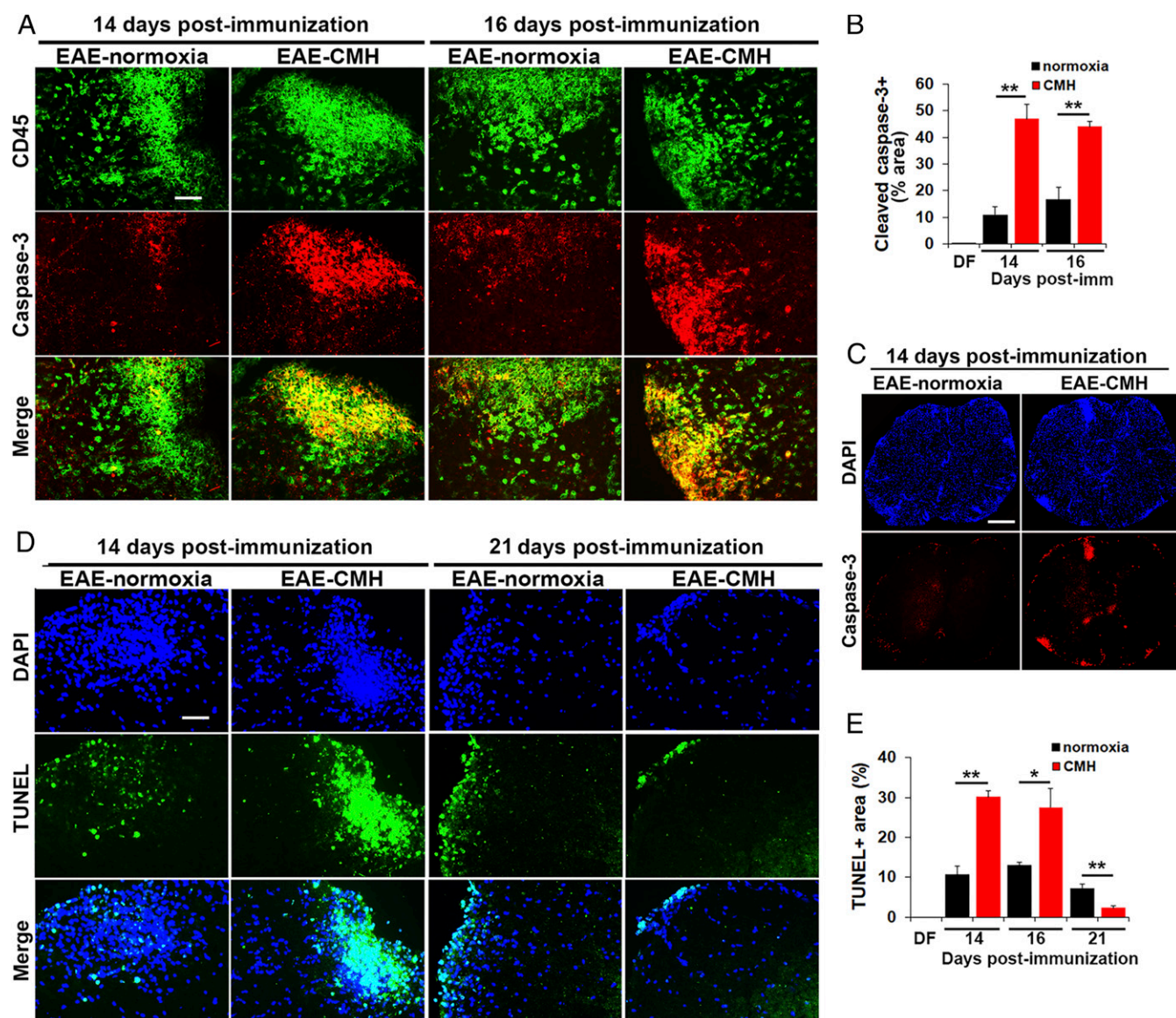
Fig. 4. CMH treatment of preexisting EAE promotes apoptosis of infiltrated leukocytes. (*A*, *C*, and *D*). Frozen sections of lumbar spinal cord taken from EAE–normoxia or EAE–CMH mice at the peak (14 and 16 d) and remission (21 d) phases of disease were stained for CD45 (AlexaFluor-488) and cleaved caspase-3 (Cy-3) in *A*, DAPI and cleaved caspase-3 (Cy-3) in *C*, or DAPI and TUNEL (AlexaFluor-488) in *D*. (Scale bar, 50 μm [*A* and *D*] and 500 μm [*C*].) (*B* and *E*) Quantification of cleaved caspase-3+ (*B*) and TUNEL+ (*E*) percent area. Results are expressed as the mean ± SEM (*n* = 6 mice per group). Note that during the peak phase of disease (days 14–16), CMH strongly enhanced the death of infiltrated leukocytes. *P < 0.05, **P < 0.01.

thereby accelerating the rate of leukocyte apoptosis. To address this question, we performed dual-IF with the monocyte marker Mac-1 and hypoxia-inducible factor 1-α (HIF-1α). As expected, this revealed no HIF-1α signal in disease-free control spinal cord, but at the peak stage of EAE, many cells stained positive for HIF-1α in inflamed spinal cord white matter, and the vast majority of these cells colocalized with the Mac-1 monocyte marker (Fig. 6*E*). Quantification revealed that at the peak of disease, spinal cords of CMH-treated mice contained significantly greater numbers of HIF-1α+ leukocytes than normoxic controls (*P* < 0.01 at 14 and 16 d postimmunization; Fig. 6*F*). These findings support the notion that CMH produces additional hypoxic stress on the already hypoxic monocytes within the EAE spinal cord, and this accelerates the rate of monocyte apoptosis.

Discussion

These studies demonstrate that when applied to preexisting inflammatory demyelinating disease, CMH (10% O$_2$) promotes clinical recovery, leading to long-term stable reductions in clinical score. Importantly, this improved clinical outcome was underpinned by marked reductions in histopathological markers of disease, including lower levels of vascular disruption, leukocyte accumulation, and demyelination. These findings are consistent with previous studies highlighting the protective influence of hypoxic preconditioning on EAE progression, but clearly have far more translational potential (8–10). In these studies, we opted to treat mice with CMH once they showed significant clinical signs (clinical score of greater than 2; i.e., significant hind limb weakness) because this is comparable to the stage of disease where a patient might present to the clinic. It is important to point out that the disease-modifying effect of CMH was not
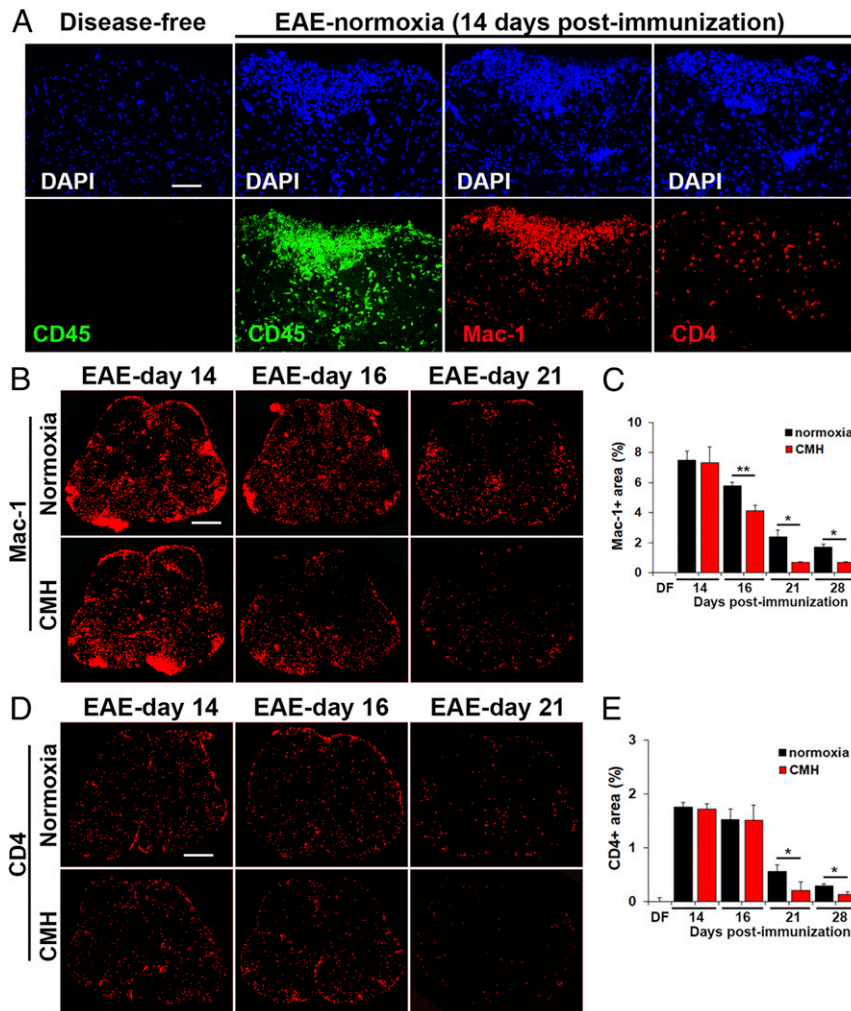
Fig. 5. Monocytes are the predominant type of leukocyte within EAE lesions. (*A*, *B*, and *D*). Frozen sections of lumbar spinal cord taken from disease-free, EAE–normoxia or EAE–CMH mice at the peak (14 and 16 d) and remission (21 d) phases of disease were stained for DAPI, CD45 (AlexaFluor-488), Mac-1 (Cy-3), or CD4 (Cy-3) in *A*, Mac-1 (Cy-3) in *B*, or CD4 (Cy-3) in *D*. (Scale bar, 50 μm [*A*] or 500 μm [*B* and *D*].) (*C* and *E*) Quantification of the total Mac-1+ (*C*) or CD4+ (*E*) area. Results are expressed as the mean ± SEM percent area (*n* = 6 mice per group). Note that during the peak phase of disease (days 14–16), monocytes are the most abundant type of leukocyte in inflammatory lesions and that CMH strongly enhanced monocyte death during the remission phase. *$P < 0.05$, **$P < 0.01$.

immediate, in that mice typically started CMH at 11 to 12 d postimmunization and over the next 3 to 4 d went on to develop similar clinical scores as their normoxic controls. However, once the remission phase began, CMH accelerated clinical recovery, resulting in long-term stable reductions in clinical score for the duration of the experiment (35 d).

The Impact of CMH on Vascular Remodeling and Integrity during EAE. Consistent with previous studies in healthy mice, CMH applied to mice with EAE stimulated a strong vascular remodeling response that was associated with enhancement of vascular integrity, as shown by reduced fibrinogen leak and underpinned by a faster reexpression of endothelial tight junction proteins during the remission phase of disease (15, 23, 24). While an angiogenic response has been described both in MS and in EAE, there is still ongoing debate as to whether angiogenic remodeling in MS is a good or bad thing (25–27). Our findings make two points. First, even in the middle of full-blown inflammatory disease, the angiogenic response triggered by CMH still proceeds, resulting in significantly increased vascular density and total vascular area. Second and perhaps even more surprising, is that by stimulating

a strong vascular remodeling response (using CMH) in the middle of ongoing inflammation, disease severity is markedly suppressed. Intuitively, one would predict that stimulating angiogenesis at this time would trigger more vascular leak as interconnecting endothelial cells uncouple from each other before migrating to form new vessels, but on the contrary, the opposite seems to happen because vessel integrity in EAE is actually enhanced. These data support the concept that angiogenesis in MS is beneficial and, by extension, suggest that other means of enhancing this angiogenic response may hold therapeutic potential in MS. This is also consistent with our recent finding that when endothelial expression of the proangiogenic fibronectin receptor, α5β1 integrin, is deleted, mice develop accelerated progression of EAE as a result of limited vascular repair (28). Our current data suggest that CMH protects in part by inducing adaptive changes in vascular integrity properties, including increased endothelial expression of tight junction proteins. Interestingly, we also found that CMH suppressed expression of endothelial VCAM-1, which via its interaction with leukocyte α4β1 integrin, plays a critical role in leukocyte extravasation into the CNS (11, 29). Importantly, this was the
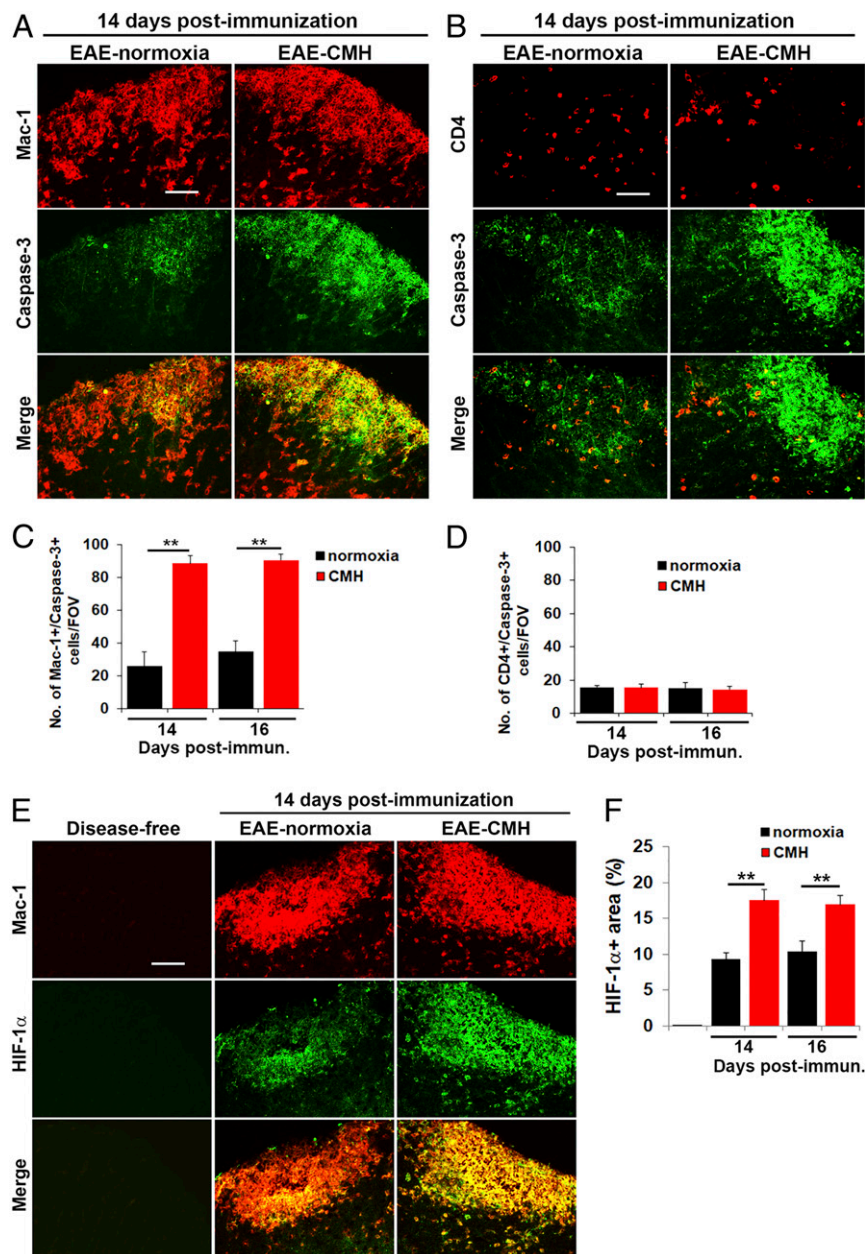
Fig. 6. CMH enhances apoptosis and HIF-1α expression in monocytes. (*A*, *B*, and *E*). Frozen sections of lumbar spinal cord taken from disease-free, EAE–normoxia or EAE–CMH mice at the peak phase of disease (14 d postimmunization) were stained for Mac-1 (Cy-3) and cleaved caspase-3 (AlexaFluor-488) in *A*, CD4 (Cy-3) and cleaved caspase-3 (AlexaFluor-488) in *B*, and Mac-1 (Cy-3) and HIF-1α (AlexaFluor-488) in *E*. (Scale bar, 25 μm.) (*C*, *D* and *F*). Quantification of the number of Mac-1/cleaved caspase-3 dual-positive (*C*) or CD4/cleaved caspase-3 dual-positive (*D*) cells/FOV or HIF-1α+ area (*F*). Results are expressed as the mean ± SEM (*n* = 6 mice per group). Note that during the peak phase of disease (days 14–16), CMH enhanced the death of infiltrated monocytes and increased HIF-1α expression in these cells. **$P < 0.01$.

earliest detectable impact of CMH treatment (significantly reduced at day 14), which would lead to suppressed leukocyte infiltration into the CNS.

In addition to enhancing vascular integrity, it is also possible that increased vascular density by itself may provide benefit by promoting increased blood flow and perfusion, thereby accelerating the removal of pathogenic stimuli from the demyelinated lesion, including myelin breakdown products and proinflammatory cytokines/chemokines that are perpetuating the inflammatory process. This concept is consistent with early therapeutic research in MS which showed that factors promoting vasodilation and increased cerebral blood flow such as amyl

nitrite and histamine offered clinical relief in the short term, a phenomenon termed "relief by flush" (30, 31).

CMH Promotes Apoptotic Clearance of Monocytes during EAE. From a mechanistic viewpoint, perhaps the most striking finding from our studies is that while in the short term (first 3 d), CMH had no obvious impact on leukocyte infiltration, during the remission phase, it strongly enhanced apoptotic removal of infiltrated monocytes from the spinal cord. Our data showing that monocytes are the most abundant type of leukocyte at all phases of EAE suggest a major role for monocytes in disease pathogenesis, consistent with the work of others (32–34). Interestingly, CMH

had a faster and more notable impact on promoting apoptosis in monocytes over CD4+ lymphocytes. While CD4+ T cells showed a fairly even distribution throughout the spinal cord white and gray matter, monocytes were often found in high-density cellular aggregates within white matter, and this was where the highest levels of HIF-1α expression and apoptotic cell death occurred. This implies that as monocytes tend to aggregate in very high-density clusters, that is where hypoxia is most severe, and so it follows that CMH will push many monocytes over the hypoxic threshold toward initiating apoptotic pathways, consistent with recent studies linking HIF-1α activation with stimulation of apoptotic pathways (35–37). A previous study showed that inhibition of caspase-mediated apoptosis prevented remission in EAE (38), in keeping with our finding that by enhancing caspase-3 activation, CMH accelerates monocyte apoptosis, thereby promoting recovery from EAE. Interestingly, our results are also consistent with previous work showing that the incidence of MS is lower at higher altitudes, where a state of relative hypoxia exists (39). Taken together, these findings provides a rationale for future therapy because while application of CMH may not be a practical solution, our data suggest that stimulating HIF-1α in monocytes by other means could provide benefit by accelerating monocyte apoptosis; e.g., stimulating HIF-1α levels either by the hypoxic mimetic cannabinoid derivative VCE-004.8 (40) or by reducing HIF-1α degradation using the prolyl hydroxylase inhibitor FG-4592 (41).

It is important to compare our findings with studies from the Smith laboratory, who demonstrated a hypoxic state in the spinal cord of EAE rodents and showed that delivery of 95% oxygen led to improvements in neurological function (20). On the face of it, our findings appear to contradict this work, so how can we rationalize the apparent contradiction that both oxygen deprivation and delivery appear to improve clinical function in EAE? We believe these differences can be explained by the timing of response as well as the molecular mechanisms underlying the effect. Because demyelinating lesions display acute hypoxia (20–22), delivery of oxygen in the short term may provide clinical benefit by helping oligodendrocytes and neurons overcome hypoxia, thereby preventing demyelination and axonal loss. However, according to our results, the downside of oxygen therapy is that it might also prevent apoptosis of hypoxic leukocytes and thus in the long term have a detrimental effect by perpetuating the inflammatory response. Unlike oxygen therapy, the application of CMH has no obvious beneficial effect in the short term (first few days), but by stimulating adaptive vasculo-protective responses and promoting apoptosis of infiltrated monocytes, it has the potential to confer extensive long-term neuroprotection. While it seems unlikely that CMH could ever be a realistic treatment option for MS patients, at the very least, this approach has proven its worth by identifying several different molecular mechanisms that might be exploitable as therapeutic options, including enhancement of vascular integrity by up-regulating tight junction proteins and by accelerating apoptosis of infiltrated monocytes. Of note, a growing number of recent studies have demonstrated the therapeutic benefit of intermittent hypoxic training (IHT) in a variety of other experimental neurological conditions, including ischemic stroke, Alzheimer's disease, spinal cord injury, and epilepsy (7, 42–44). Thus, in future studies, in addition to pursuing the mechanisms identified here, we will determine whether IHT confers similar benefit in EAE, define the level of hypoxia that is required to mediate protection, and also examine whether this protection is sex-specific.

Materials and Methods

Animals. The studies described here were approved by Institutional Animal Care and Use Committees of the Scripps Research Institute (TSRI) and Explora Biolabs at San Diego Biomedical Research Institute (SDBRI). Wild-type female SJL/J mice were obtained from Jackson Laboratories and maintained under pathogen-free conditions in the closed breeding colonies of TSRI and SDBRI.

Experimental Autoimmune Encephalomyelitis. As previously described, EAE was performed using a standard protocol and materials provided by Hooke Laboratories (10). Briefly, 10-wk-old SJL/J female mice, housed five to a cage, were immunized s.c. with 200 μL of 1 mg/mL PLP$_{139-151}$ peptide emulsified in complete Freund's adjuvant containing 1 mg/mL *Mycobacterium tuberculosis* in the base of the tail and upper back. This protocol leads to strong and consistent induction of clinical EAE in which mice reach peak disease typically 14 d postimmunization before making significant recovery between days 18 and 28 (remission), before following a cyclical relapsing–remitting course (45, 46). Mice were evaluated daily for clinical signs and scored according to the following rubric: 0, no symptoms; 1, flaccid tail; 2, paresis of hind limbs; 3, paralysis of hind limbs; 4, quadriplegia; 5, death. Clinical EAE data were assessed using one-way ANOVA followed by post hoc Student's *t* test, in which $P < 0.05$ was defined as statistically significant. For analysis of histological parameters, disease-free controls or EAE mice maintained under normoxic or hypoxic conditions were euthanized after 14, 16, 21, 28, and 35 d postimmunization and samples harvested.

Chronic Hypoxia Model. After immunization with PLP$_{139-151}$ peptide, once mice developed a clinical score of 2 or greater (typically 10–11 d post-immunization), they were randomly assigned to one of two groups (housed five to a cage): one was placed into a chamber (Biospherix) maintained under hypoxic conditions (10% O_2) for the duration of the experiment, while the other (control) group was kept under normoxic conditions (~21% O_2 at sea level) in the same room. Every few days, the chamber was briefly opened for cage cleaning and food and water replacement as needed.

Immunohistochemistry and Antibodies. Immunohistochemistry was performed on 10 μm frozen sections of cold phosphate buffer saline perfused tissues as described previously (10). DAPI-containing mounting medium was obtained from Sigma. The following rat monoclonal antibodies (BD Pharmingen) were used in this study: CD31 (clone MEC13.3; 1:500), VCAM-1 (clone 429; 1:100), CD45 (1:300), and Mac-1 (clone M1/70; 1:100). The rat monoclonal antibody reactive for CD4 (clone GK1.5; 1:300) was obtained from R&D Systems. The hamster anti-CD31 monoclonal antibody (clone 2H8; 1:500) was obtained from Abcam. The following rabbit polyclonal antibodies were also used: occludin and ZO-1 (1:2,000 from Invitrogen), fibrinogen (1:2,000 from Millipore), and hypoxia-inducible factor-1α (1:500 from Novus Biologicals). Anticleaved caspase-3 antibodies (rabbit polyclonal and monoclonal [clone 5A1E]) were used at 1:500 and obtained from Cell Signaling Technology. Fluoromyelin-red (1:50) was obtained from Invitrogen. Secondary antibodies used (all at 1:500 dilution) included Cy3-conjugated anti-rat, anti-rabbit, and anti-goat from Jackson Immunoresearch and Alexa Fluor 488-conjugated anti-rat, anti-hamster, and anti-rabbit from Invitrogen. TUNEL staining was performed using the TUNEL kit (Invitrogen) according to manufacturer's instructions.

Image Analysis. Images were taken on a Keyence 710 fluorescent microscope using a 2×, 10×, 20×, or 40× objective. Analysis was performed in the lumbar region of the spinal cord. In all analyses, at least three randomly selected areas were captured at 10× or 20× magnification per tissue section and three sections per spinal cord analyzed to calculate the mean for each subject. For every antigen in each experiment, exposure time was selected to transmit the maximum amount of information without saturating the image, and this was kept constant for each antigen across the different experimental conditions. As Mac-1 is expressed both by monocytes (high levels) and microglia (low levels), when taking images of this marker, we used short exposure times to specifically capture the monocyte signal but exclude the weaker signal contributed by microglia. The degree of infiltration of leukocytes (CD45+), monocytes (Mac-1), CD4+ lymphocytes, or fibrinogen leakage was evaluated by NIH Image J software to provide a measure of total fluorescent area per field of view (FOV). To quantify the fluorescent area of the cleaved caspase-3, HIF-1α, or TUNEL+ antigens, images were specifically captured of infiltrated leukocyte aggregates and the fluorescent area of each antigen within these specific fields measured. Numbers of Mac-1+/cleaved caspase-3+ or CD4+/cleaved caspase-3+ dual-positive cells/FOV were quantified by counting using Image J software. The number of blood vessels expressing VCAM-1 per FOV or the percent of vessels expressing the tight junction proteins ZO-1 and occludin was evaluated by capturing images and counted using Image J software. Vascularity was evaluated in an unbiased automated manner in four consecutive serial sections per spinal cord using Image J software to provide both a measure of vessel density (number

of blood vessels/FOV) and total vascular area (percent area covered by CD31+ blood vessels). Based on a priori power analysis using G*Power software, we used minimum cohort sizes of six animals per group, and the results were expressed as the mean ± SEM (47). Statistical significance was assessed using one-way ANOVA followed by Tukey's multiple comparison post hoc test, in which $P < 0.05$ was defined as statistically significant.

1. A. Doshi, J. Chataway, Multiple sclerosis, a treatable disease. *Clin. Med. (Lond.)* **17**, 530–536 (2017).
2. D. M. Wingerchuk, J. L. Carter, Multiple sclerosis: Current and emerging disease-modifying therapies and treatment strategies. *Mayo Clin. Proc.* **89**, 225–240 (2014).
3. C. Ffrench-Constant, Pathogenesis of multiple sclerosis. *Lancet* **343**, 271–275 (1994).
4. H. Lassmann, "Multiple sclerosis pathology" in *McAlpine's Multiple Sclerosis*, A. Compston, Ed. (Churchill Livingstone, ed. 3, 1998), pp. 323–358.
5. J. Dowden, D. Corbett, Ischemic preconditioning in 18- to 20-month-old gerbils: Long-term survival with functional outcome measures. *Stroke* **30**, 1240–1246 (1999).
6. B. A. Miller *et al.*, Cerebral protection by hypoxic preconditioning in a murine model of focal ischemia-reperfusion. *Neuroreport* **12**, 1663–1669 (2001).
7. A. M. Stowe, T. Altay, A. B. Freie, J. M. Gidday, Repetitive hypoxia extends endogenous neurovascular protection for stroke. *Ann. Neurol.* **69**, 975–985 (2011).
8. P. Dore-Duffy, M. Wencel, V. Katyshev, K. Cleary, Chronic mild hypoxia ameliorates chronic inflammatory activity in myelin oligodendrocyte glycoprotein (MOG) peptide induced experimental autoimmune encephalomyelitis (EAE). *Adv. Exp. Med. Biol.* **701**, 165–173 (2011).
9. N. Esen, V. Katyshev, Z. Serkin, S. Katysheva, P. Dore-Duffy, Endogenous adaptation to low oxygen modulates T-cell regulatory pathways in EAE. *J. Neuroinflammation* **13**, 13 (2016).
10. S. K. Halder, R. Kant, R. Milner, Hypoxic pre-conditioning suppresses experimental autoimmune encephalomyelitis by modifying multiple properties of blood vessels. *Acta Neuropathol. Commun.* **6**, 86 (2018).
11. S. J. Lee, E. N. Benveniste, Adhesion molecule expression and regulation on cells of the central nervous system. *J. Neuroimmunol.* **98**, 77–88 (1999).
12. P. Ballabh, A. Braun, M. Nedergaard, The blood-brain barrier: An overview: Structure, regulation, and clinical implications. *Neurobiol. Dis.* **16**, 1–13 (2004).
13. J. D. Huber, R. D. Egleton, T. P. Davis, Molecular physiology and pathophysiology of tight junctions in the blood-brain barrier. *Trends Neurosci.* **24**, 719–725 (2001).
14. J. C. LaManna, L. M. Vendel, R. M. Farrell, Brain adaptation to chronic hypobaric hypoxia in rats. *J. Appl. Physiol.* **72**, 2238–2243 (1992).
15. R. Milner *et al.*, Increased expression of fibronectin and the α 5 β 1 integrin in angiogenic cerebral blood vessels of mice subject to hypobaric hypoxia. *Mol. Cell. Neurosci.* **38**, 43–52 (2008).
16. S. Issazadeh *et al.*, Role of passive T-cell death in chronic experimental autoimmune encephalomyelitis. *J. Clin. Invest.* **105**, 1109–1116 (2000).
17. M. Schmied *et al.*, Apoptosis of T lymphocytes in experimental autoimmune encephalomyelitis. Evidence for programmed cell death as a mechanism to control inflammation in the brain. *Am. J. Pathol.* **143**, 446–452 (1993).
18. J. A. Lyons, M. J. Ramsbottom, R. J. Mikesell, A. H. Cross, B cells limit epitope spreading and reduce severity of EAE induced with PLP peptide in BALB/c mice. *J. Autoimmun.* **31**, 149–155 (2008).
19. D. Sun *et al.*, Myelin antigen-specific CD8+ T cells are encephalitogenic and produce severe disease in C57BL/6 mice. *J. Immunol.* **166**, 7579–7587 (2001).
20. A. L. Davies *et al.*, Neurological deficits caused by tissue hypoxia in neuroinflammatory disease. *Ann. Neurol.* **74**, 815–825 (2013).
21. T. W. Johnson *et al.*, Gray matter hypoxia in the brain of the experimental autoimmune encephalomyelitis model of multiple sclerosis. *PLoS One* **11**, e0167196 (2016).
22. R. Yang, J. F. Dunn, Reduced cortical microvascular oxygenation in multiple sclerosis: A blinded, case-controlled study using a novel quantitative near-infrared spectroscopy method. *Sci. Rep.* **5**, 16477 (2015).
23. J. C. LaManna, N. T. Kuo, W. D. Lust, Hypoxia-induced brain angiogenesis. Signals and consequences. *Adv. Exp. Med. Biol.* **454**, 287–293 (1998).
24. L. Li *et al.*, In the hypoxic central nervous system, endothelial cell proliferation is followed by astrocyte activation, proliferation, and increased expression of the α 6 β 4 integrin and dystroglycan. *Glia* **58**, 1157–1167 (2010).
25. A. Boroujerdi, J. V. Welser-Alves, R. Milner, Extensive vascular remodeling in the spinal cord of pre-symptomatic experimental autoimmune encephalomyelitis mice; increased vessel expression of fibronectin and the α5β1 integrin. *Exp. Neurol.* **250**, 43–51 (2013).
26. J. E. Holley, J. Newcombe, J. L. Whatmore, N. J. Gutowski, Increased blood vessel density and endothelial cell proliferation in multiple sclerosis cerebral white matter. *Neurosci. Lett.* **470**, 65–70 (2010).
27. T. J. Seabrook *et al.*, Angiogenesis is present in experimental autoimmune encephalomyelitis and pro-angiogenic factors are increased in multiple sclerosis lesions. *J. Neuroinflammation* **7**, 95 (2010).
28. R. Kant, S. K. Halder, G. J. Bix, R. Milner, Absence of endothelial α5β1 integrin triggers early onset of experimental autoimmune encephalomyelitis due to reduced vascular remodeling and compromised vascular integrity. *Acta Neuropathol. Commun.* **7**, 11 (2019).
29. T. A. Yednock *et al.*, Prevention of experimental autoimmune encephalomyelitis by antibodies against α 4 β 1 integrin. *Nature* **356**, 63–66 (1992).
30. R. M. Brickner, Pharmacological reduction of abnormality in multiple sclerosis within minutes: A statistical study. *J. Nerv. Ment. Dis.* **127**, 308–322 (1958).
31. H. D. Jonez, Multiple sclerosis; treatment with histamine and d-tubocurarine. *Ann. Allergy* **6**, 550–563 (1948).
32. B. Ajami, J. L. Bennett, C. Krieger, K. M. McNagny, F. M. Rossi, Infiltrating monocytes trigger EAE progression, but do not contribute to the resident microglia pool. *Nat. Neurosci.* **14**, 1142–1149 (2011).
33. M. A. Moreno *et al.*, Therapeutic depletion of monocyte-derived cells protects from long-term axonal loss in experimental autoimmune encephalomyelitis. *J. Neuroimmunol.* **290**, 36–46 (2016).
34. J. C. Nissen, K. K. Thompson, B. L. West, S. E. Tsirka, Csf1R inhibition attenuates experimental autoimmune encephalomyelitis and promotes recovery. *Exp. Neurol.* **307**, 24–36 (2018).
35. M. P. Biju *et al.*, Vhlh gene deletion induces Hif-1-mediated cell death in thymocytes. *Mol. Cell. Biol.* **24**, 9038–9047 (2004).
36. S. Krick *et al.*, Role of hypoxia-inducible factor-1alpha in hypoxia-induced apoptosis of primary alveolar epithelial type II cells. *Am. J. Respir. Cell Mol. Biol.* **32**, 395–403 (2005).
37. F. Luo *et al.*, Hypoxia-inducible transcription factor-1α promotes hypoxia-induced A549 apoptosis via a mechanism that involves the glycolysis pathway. *BMC Cancer* **6**, 26 (2006).
38. Y. Okuda, S. Sakoda, H. Fujimura, T. Yanagihara, The effect of apoptosis inhibitors on experimental autoimmune encephalomyelitis: Apoptosis as a regulatory factor. *Biochem. Biophys. Res. Commun.* **267**, 826–830 (2000).
39. J. F. Kurtzke, On the fine structure of the distribution of multiple sclerosis. *Acta Neurol. Scand.* **43**, 257–282 (1967).
40. C. Navarrete *et al.*, Hypoxia mimetic activity of VCE-004.8, a cannabidiol quinone derivative: Implications for multiple sclerosis therapy. *J. Neuroinflammation* **15**, 64 (2018).
41. I. H. Jain *et al.*, Hypoxia as a therapy for mitochondrial disease. *Science* **352**, 54–61 (2016).
42. D. D. Fuller, S. M. Johnson, E. B. J. Olson, Jr, G. S. Mitchell, Synaptic pathways to phrenic motoneurons are enhanced by chronic intermittent hypoxia after cervical spinal cord injury. *J. Neurosci.* **23**, 2993–3000 (2003).
43. E. B. Manukhina *et al.*, Prevention of neurodegenerative damage to the brain in rats in experimental Alzheimer's disease by adaptation to hypoxia. *Neurosci. Behav. Physiol.* **40**, 737–743 (2010).
44. J. L. Zhen *et al.*, Chronic intermittent hypoxic preconditioning suppresses pilocarpine-induced seizures and associated hippocampal neurodegeneration. *Brain Res.* **1563**, 122–130 (2014).
45. B. L. McRae *et al.*, Induction of active and adoptive relapsing experimental autoimmune encephalomyelitis (EAE) using an encephalitogenic epitope of proteolipid protein. *J. Neuroimmunol.* **38**, 229–240 (1992).
46. B. L. McRae, C. L. Vanderlugt, M. C. Dal Canto, S. D. Miller, Functional evidence for epitope spreading in the relapsing pathology of experimental autoimmune encephalomyelitis. *J. Exp. Med.* **182**, 75–85 (1995).
47. F. Faul, E. Erdfelder, A. Buchner, A. G. Lang, Statistical power analyses using G*power 3.1: Tests for correlation and regression analyses. *Behav. Res. Methods* **41**, 1149–1160 (2009).

NEUROSCIENCE